Int. J. Electrochem. Sci., 17 **(2022)** Article Number: 220956, doi: 10.20964/2022.09.54

International Journal of
ELECTROCHEMICAL
SCIENCE
www.electrochemsci.org

Eco-friendly Ginkgo Leaf Extract as a Green Corrosion Inhibitor to Protect N80 Steel in 1 M HCl

Yingmei Zhou[1], *Zhengnan Wei*[2,*] , *Hui Zhi*[3,*], *Yue Wang*[4], *Xiuquan Yao*[3]

[1] School of Chemical Engineering, Shandong Institute of Petroleum and Chemical Technology, Dongying, 257601, China
[2] Novel Energy Development Center of Shengli Petroleum Administration, SINOPEC, Dongying 257000, China
[3] National Center for Materials Service Safety, University of Science and Technology Beijing, Beijing, 100083, China
[4] Institute for Advanced Materials and Technology, University of Science and Technology Beijing, Beijing, 100083, China
[*]E-mail: g20209167@xs.ustb.edu.cn; 18653477681@163.com

Received: 3 May 2022 / *Accepted:* 30 June 2022 / *Published:* 7 August 2022

Developing efficient and green corrosion inhibitors is a general trend to replace traditional toxic and harmful corrosion inhibitors, which is not an exception in the corrosion protection and pickling industry in the petroleum industry. Herein, we prepared ginkgo leaf extract (GE) as a green corrosion inhibitor by one-step water extraction. We demonstrated the anti-corrosion performance of GE on N80 steel by combining experiments and calculations. The electrochemical results showed that GE could slow down the corrosion of N80 steel in acidic environment by improving its charge transfer resistance and inhibiting its cathodic and anodic reactions. The weight loss experiments were consistent with the electrochemical test results. We explained the interaction mechanism between GE and N80 steel from the microscopic level based on the Langmuir adsorption model and computer simulation. In short, the 6-hydroxykynurenic acid molecule (from GE) was adsorbed on the surface of N80 steel through benzene rings and heteroatoms in parallel and offered excellent anti-corrosion performance for N80 steel.

Keywords: Green corrosion inhibitor, Plant extract, EIS, Weight loss, MD simulation

1. INTRODUCTION

Petroleum is a viscous, dark brown liquid known as the "blood of the industry." Petroleum is mainly used as fuel oil and gasoline and is one of the most important primary energy sources in the world. At the same time, it is also the raw material for many chemical industry products, such as solutions, fertilizers, pesticides, and plastics. There is no doubt that petroleum promotes the prosperity

and development of industry and contributes to social progress [1-3]. However, the reserve of crude oil is limited, and the crude output of many oilfields gradually declines after a long period of exploitation. Based on the above reason, the depth of oilfields extraction has increased, and the extraction environment has become more severe. That is to say, the acidity of the extracted crude oil increases, which aggravates the corrosion rate of the extraction equipment and oil pipelines. Meanwhile, corrosion also caused huge security risks and economic losses. Therefore, it is urgent to develop efficient, convenient, cheap, and practical anti-corrosion technologies [4-6].

Among many anti-corrosion technologies, corrosion inhibitors are known for their low dosage, immediate effect, low cost, and ease of use [7]. Corrosion inhibitor is also an indispensable additive in the pickling process because they can effectively slow down the corrosion of metals. Based on different components, corrosion inhibitors can be divided into inorganic corrosion inhibitors and organic corrosion inhibitors. As the name suggests, inorganic corrosion inhibitors are mainly based on inorganic substances, such as chromate, nitrite, and phosphate. Once people's awareness of environmental protection was weak, inorganic corrosion inhibitors were widely used. Organic corrosion inhibitors are mainly composed of organic substances, such as imidazoles, thiazoles, and triazoles. Organic corrosion inhibitors all have a common feature, that is, they have N atom, O atom, S atom, P atom, benzene rings, and non-polar covalent bonds [8]. Organic corrosion inhibitors can be adsorbed on the metal surface through chemical or physical acting force under the gain and loss of electrons or electrostatic forces [9]. Haque synthesized two kinds of imidazolium zwitterion and explored the corrosion inhibition performance of imidazolium on mild steel in acidic environment (1 M HCl) [10]. Hydroxyl-containing zwitterion and sulphur containing zwitterion showed 94.9% (50 ppm) and 94.9% (2 ppm) anti-corrosion ability, respectively. The excellent anti-corrosion performance was attributed to heteroatoms physical/chemical adsorption in two imidazolium zwitterion on the metal surface, such as N atom, O atom, and S atom. Based on the work of El-Lateef, the corrosion inhibition of salycilidene isatin hydrazine sodium sulfonate for carbon steel in HCl was demonstrated by the adsorption of heteroatoms [11-13]. But with the concept of sustainable development, researchers hope to develop green, efficient, easily accessible, and biodegradable corrosion inhibitors.

Plant extracts, which contain various organic compounds (ketones, aldehydes, and azoles) and are derived from nature, are potential green corrosion inhibitors [14]. Therefore, the research on plant extracts as corrosion inhibitors has triggered a research upsurge. Li prepared cauliflower extract and explored its corrosion inhibition performance on Q235 steel in two typical acid environments [15]. The electrochemical results showed that the corrosion inhibition efficiencies of cauliflower extract to Q235 steel in acidic environments were more than 90%, which was consistent with the weight loss result. Based on atomic-scale/DFT-theoretical simulations & electrochemical assessments, Shahini explored the anti-corrosion properties of *chamomile flower* extract in the hydrochloric acid solution for mild steel [16]. The results indicated that *chamomile flower* extract can provide protection for steel through parallel adsorption.

Although many plant extract inhibitors have been developed, few works exist on extract corrosion inhibitors for anti-corrosion oil pipelines. To promote the application of extract inhibitor in oil pipelines, we prepared ginkgo leaf extract (GE) by one-step pure water extraction and explored its anti-corrosion performance on N80 steel in 1 M HCl solution. In this work, weight loss, electrochemical

impedance spectroscopy (EIS), the potentiodynamic polarization curve, atomic force microscope (AFM), and scanning electron microscope (SEM) were employed to explore the inhibition performance of ginkgo leaf extract for N80 steel. Then, the molecular simulation (MD) was used to demonstrate the anti-corrosion mechanism of GE for N80 steel.

2. EXPERIMENTAL

2.1 Materials

The N80 steel came from the Shengli Oilfield, a subsidiary of Sinopec Group Corporation. The percentage weight composition of N80 steel grade is: 0.31% C, 0.19% Si, 0.92% Mn, 0.01% P, 0.008% S, 0.2% Cr, and balance Fe. The sample size used for electrochemical testing was 1×1×1 cm^3, except for a work surface (1×1 cm^2), other surfaces were sealed by epoxy resin. The 1 M HCl solution used for the test was prepared from concentrated hydrochloric acid (37 wt%) and deionized water.

Ginkgo leaf extract was prepared via a water extraction, which referred Qiang extract method [17]. In short, the washed fresh ginkgo leaves were dried and crushed. Then, it was transferred to a 3 L beaker containing 1.4 L deionized water and boiled for 12 h. Next, the cloudy liquid was filtered after cooling to room temperature. Finally, the liquid obtained by filtration was freeze-dried for 24 h and then put into a vacuum desiccator for use. The added concentrations of GE in the HCl solution were 100, 200, 400, and 800 mg/L. The blank test solution in this work was 1 M HCl.

2.2 Electrochemical tests

Electrochemical measurements were performed using a conventional three-electrode system, including a working electrode (N80 steel), a counter electrode (1 cm^2 platinum sheet), and a reference electrode (saturated calomel electrode). The electrochemical workstation used in this work was CHI760E (Shanghai Chenhua). The tested range of EIS was 10^5 Hz to 10^{-2} Hz, and the sinusoidal perturbation potential was 5 mV. After that, the Potentiodynamic polarization curves was carried out. Here, the potential scanning interval was ±250 mV (based on self-corrosion potential), and the scanning rate was 2 mV/s. To ensure the accuracy of the electrochemical results, all tests were repeated.

2.3 Weight loss

The N80 steel samples for the immersion test were executed in terms of the ASTM standard G 31-72. N80 steel was put in the 1 M HCl containing various concentrations of GE (0, 100, 200, 400, 800 ml/L) for 10 h. Then, the immersed steel was washed with ethyl alcohol several times and then dried via an air blower. The N80 steel specimens were weighed before and after immersion. Finally, relevant data were recorded and discussed.

2.4 Surface characterization

The sample sizes used for SEM (JEOL-JSM-7800F) and AFM (MFP-3D-BIO) were 1×1×0.3 cm^3 and 0.5×0.5×0.2 cm^3. Except for the blank solution for comparison, the same samples were also immersed in 800 ml/L ginkgo leaf extract solution. Before soaking, all samples were polished with different emery paper (400, 800, 2000, and 7000 mesh). The sample used for SEM was immersed for 8 h and used for AFM was 4 h. After soaking, all samples were ultrasonically cleaned with ethanol several times and then dried with a blower.

2.5 Molecular simulation

Due to the complex composition of ginkgo leaf extract, we selected one molecule (6-hydroxykynurenic acid, HKA) of the active ingredients for MD calculation. Based on the Forcite module of the MD, the microcosmic level interaction mechanism between HKA and N80 steel was studied. The simulation cell size was 28.7 × 18.8 × 69.8 Å, which contained 4 frozen Fe (110) layers, 1 HKA molecule, and 300 H_2O [18]. The simulation was performed under the COMPASS force field and periodic boundary conditions [19, 20]. The total emulation time was 500 ps, and the step size was 1 fs under NVT canonical ensemble.

3. RESULTS AND DISCUSSION

3.1 EIS analysis

The EIS results of N80 steel in various concentrations of ginkgo leaf extract were shown in Fig. 1. The impedance value of the N80 steel in the blank solution was very small, which indicated that the bare N80 steel was difficult to resist the erosion of the HCl solution.

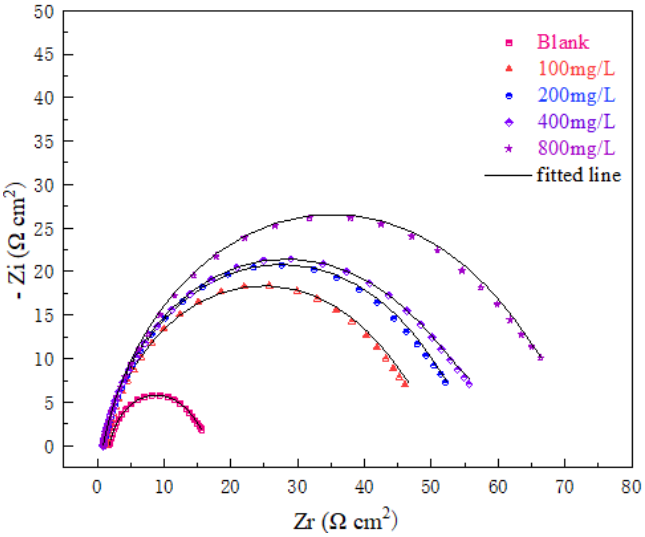

Figure 1. Nyquist plots of N80 steel in 1M HCl soultion with various concentrations of ginkgo leaf extract (0 mg/L, 100 mg/L, 200 mg/L, 400 mg/L, 800 mg/L) at 298K.

Fortunately, ginkgo leaf extract appearance significantly increased the impedance of N80 steel, and this phenomenon became more obvious with the increase of ginkgo leaf extract concentration. The Nyquist plot expanded significantly, especially when the amount of GE added reached 800 mg/L. These phenomena showed that the appearance of GE could effectively enhance the corrosion resistance of N80 steel. The appearance of GE did not affect the shape of the Nyquist plots, which indicated that GE could not affect the reaction mechanism of N80 steel in HCl solution. However, all Nyquist plots exhibited a suppressed arc called frequency dispersion. Although the cause of the frequency dispersion was uncertain, it is certainly related to the solution conductivity, the N80 steel surface morphology, and the GE adsorption layer [21].

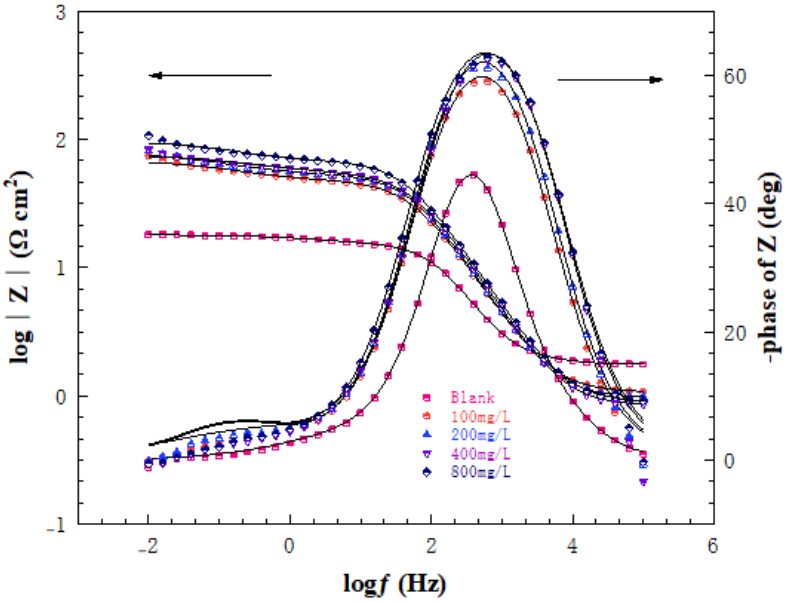

Figure 2. Bode and phase angle plots of N80 steel in 1M HCl soultion with various concentrations of ginkgo leaf extract (0 mg/L, 100 mg/L, 200 mg/L, 400 mg/L, 800 mg/L) at 298K.

Corresponding Bode and phase angle plots of N80 steel in various concentrations of ginkgo leaf extract were shown in Fig. 2. The low-frequency impedance modulus value increased with increasing GE concentration. The 800 mg/L GE showed the highest impedance modulus value, about an order of magnitude higher than blank. Meanwhile, the phase angle also became taller and wider with increasing GE concentration than blank. These findings indicated that GE could effectively improve the corrosion resistance of N80 steel in 1 M HCl solution.

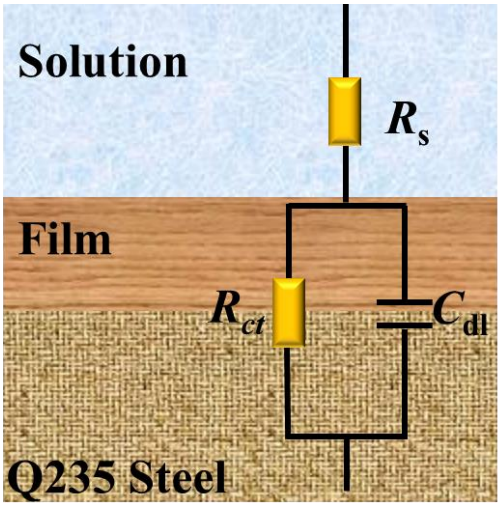

Figure 3. The equivalent circuit was used to fit the EIS data in Figures 1 and 2.

An equivalent circuit was used to fit the obtained EIS data and given in Fig. 3. Some important parameters such as Rc (solution resistance), Rct (charge transfer resistance), and Cdl (electric double layer capacitance) were obtained and shown in Table 1 [22].

Table 1. EIS parameters of N80 steel in 1M HCl soultion with various ginkgo leaf extract concentrations (0 mg/L, 100 mg/L, 200 mg/L, 400 mg/L, 800 mg/L) at 298K.

C(mg/L)	Rs(Ω cm^2)	Rct(Ω cm^2)	Cdl(μF cm^{-2})	n	η（%）
Blank	0.8	16.4	256.3	0.86	-
100	1.1	52.1	162.1	0.84	68.5
200	1.1	57.6	124.2	0.75	71.5
400	1.8	61.3	103.5	0.73	73.2
800	2.4	73.5	97.2	0.88	77.7

With the increase in GE concentration, the value of Rct increased from 16.4 Ω cm^2 to 73.5 Ω cm^2, implying that the adsorption of GE increased the difficulty of charge transfer [23]. In addition, the value of Cdl decreased from 256.3 μF cm^{-2} to 97.2 μF cm^{-2} with the increase in GE concentration, indicating that GE formed an adsorption film on the surface of N80 steel.

3.2 Potentiodynamic polarization curves

The Potentiodynamic polarization curves plots of N80 steel in various concentrations of ginkgo leaf extract were presented in Fig. 4. As shown in Fig. 4, the appearance of GE significantly reduced the cathodic and anodic polarization curves of N80 steel in HCl. Moreover, this phenomenon became more obvious with the increase in GE concentration. Obviously, GE could effectively inhibit the cathodic and anodic reaction of N80 steel in hydrochloric acid solution. This finding could be attributed to a protective layer formed on the N80 steel surface by the active components in GE, and this protective layer became denser with the increase in GE concentration [24, 25]. Compared with the anodic curve of

Potentiodynamic polarization curves containing GE, the cathodic curve had a more obvious downward shift, which indicated that GE presented a stronger inhibitory effect on the cathodic reaction of N80 steel. The shapes of all Potentiodynamic polarization curves did not change significantly, which indicated that the reaction mechanism of N80 steel in 1 M HCl solution did not change by the GE film.

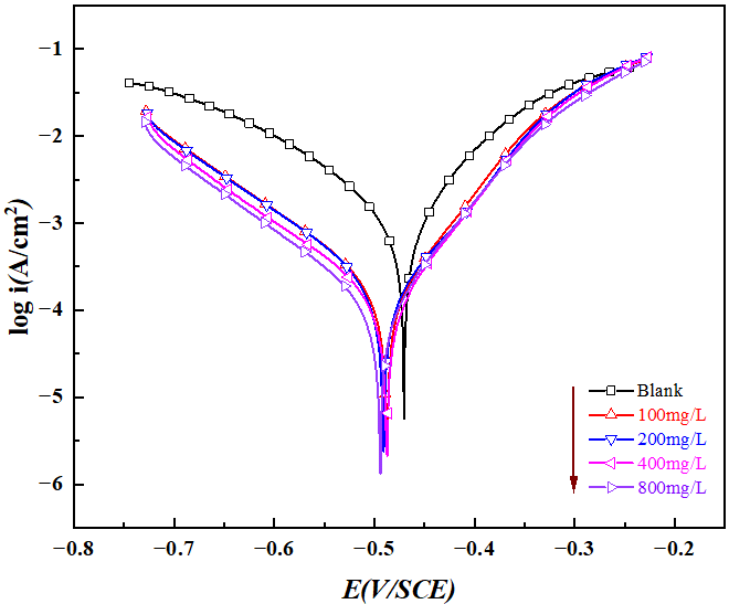

Figure 4. Potentiodynamic polarization curves plot of N80 steel in 1M HCl soultion with various concentrations of ginkgo leaf extract (0 mg/L, 100 mg/L, 200 mg/L, 400 mg/L, 800 mg/L) at 298K.

Table 2. Potentiodynamic polarization curves parameters of N80 steel in 1M HCl with various ginkgo leaf extract concentrations (0 mg/L, 100 mg/L, 200 mg/L, 400 mg/L, 800 mg/L) at 298K.

C(mg/L)	Ecorr （mV/SCE）	icorr （μAcm^{-2}）	β_a (mV dec^{-1})	β_c (mV dec^{-1})	η （%）
Blank	-479	1193	102	-124	-
100	-479	358	66	-120	70.0
200	-477	295	69	-117	75.3
400	-485	276	73	-122	76.9
800	-487	248	70	-129	79.2

By extrapolating the Potentiodynamic polarization curves, some key data parameters, such as Ecorr, icorr, anodic and cathodic Tafel slope (βa and βc), were obtained and given in Table 2. As shown in Table 2, compared with the blank, the N80 steel self-corrosion potential value change did not exceed 85mV in different GE solutions [26]. This phenomenon showed that GE was a modest mixed-type corrosion inhibitor. It was worth noting that the presence of GE significantly reduced the current density of N80 steel, which indicated that the corrosion rate of N80 steel in acidic solution was reduced. On the contrary, the η value of N80 steel increased with the increase of GE concentration, and the highest η

value was 79.2%, which further proved that GE could provide efficient protection for N80 steel [27]. The value of βa and βc did not change clearly, consistent with the EIS results. That is, the adsorption of GE did not affect the reaction mechanism of N80 steel [28].

Table 3 presents some references in recent years about plant extracts as corrosion inhibitors. It can be found from Table 3 that some of their highest corrosion inhibition efficiency values were high than that of CE for N80 steel. However, their usage was large, and the cost was high. Therefore, it can be shown that CE is an excellent performance corrosion inhibitor for N80 steel in 1 M HCl.

Table 3. Some representative references of plant extracts in recent years.

Inhibitor	**Metal**	**Concentration**	**Acid**	***η* (%)**
This work	N80 steel	0.8 g/L	1 M HCl	79.2
E. aegyptiaca [29]	Cast iron	2400 ppm	1 M HCl	91.4
watermelon seed [30]	Mild steel	2 g/L	1 M HCl	83.7
Rollinia occidentalis [31]	Mild steel	1 g/L	1 M HCl	79.7
Date Palm Seed [32]	Mild steel	2.5 g	0.5 M H_2SO_4	78.9
Malpighia glabra leaf [33]	Carbon steel	0.5 g/L	1 M HCl	69.0
winged bean extracts [34]	reinforced steel	100 ppm	1 M HCl	45.2

3.3 Weight loss

Weight loss is regarded as the most direct and traditional method for evaluating metal corrosion degree. Herein, the weight loss data of N80 steel in various concentrations of GE were obtained and presented in Fig. 5. As shown in Fig. 4, the corrosion rate of N80 steel in 1 M HCl was 28.7 mg $m^{-2}h^{-1}$, which was much higher than N80 steel in 1 M HCl with 100 mg/L GE (14.6 mg $m^{-2}h^{-1}$). Interestingly, the corrosion rate of N80 steel continued to decrease with the increase in GE concentration. This finding indicated that the increase of GE concentration promoted the adsorption of more active ingredients in GE on the metal surface, making the entire protective film denser [35]. This result was also why the corrosion rate of N80 steel in 800 mg/L GE was the smallest (9.2 mg $m^{-2}h^{-1}$).

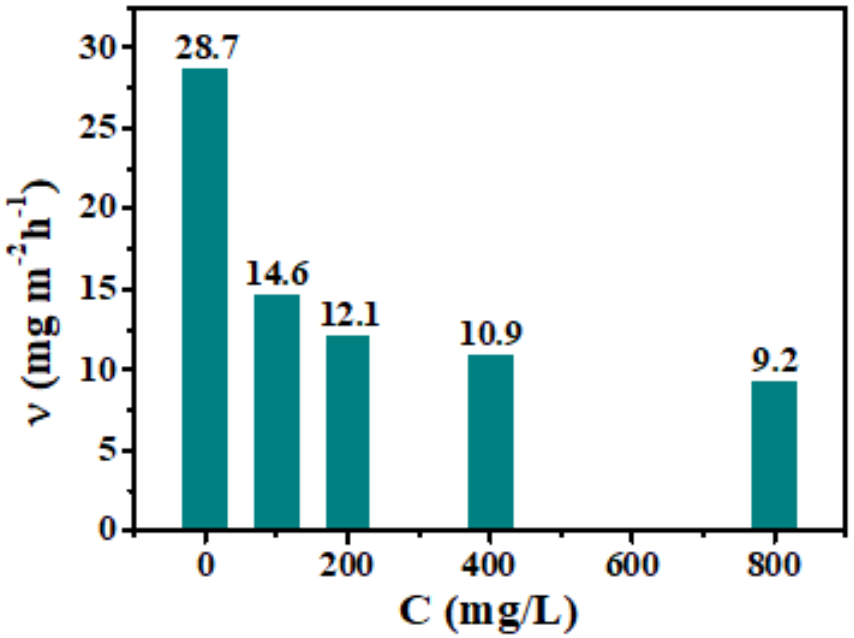

Figure 5. The weight loss rate of N80 steel in 1M HCl with various concentrations of ginkgo leaf extract (0 mg/L, 100 mg/L, 200 mg/L, 400 mg/L, 800 mg/L) at 298K.

3.4 SEM and AFM analysis

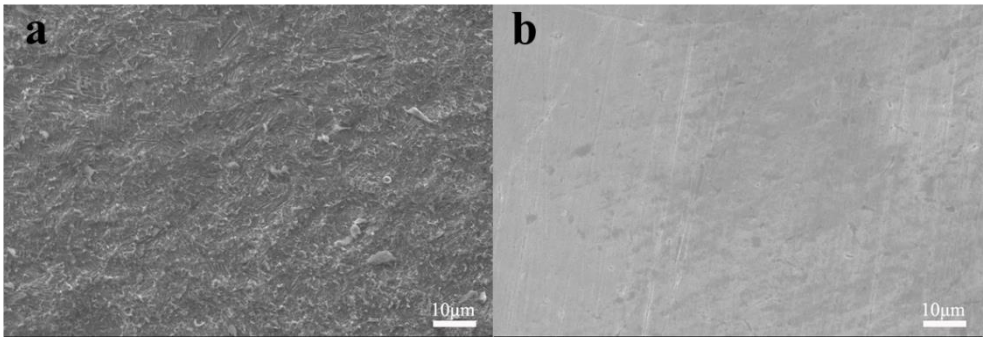

Figure 6. The SEM graphs of N80 steel in 1 M HCl with various concentrations of ginkgo leaf extract (0 mg/L, 800 mg/L) at 298K.

The SEM and AFM graphs of N80 steel in blank HCl and 800 mg/L GE solution were presented in Figs. 6 and 7. As shown in Fig. 6a, the N80 steel surface was covered with corrosion products, and many pits and protrusions appeared, which indicated that N80 steel was hard to resist the erosion of corrosive ions. This finding was consistent with previous electrochemical results. Compared with Fig. 6a, the surface morphology of N80 steel (Fig. 6b) in HCl solution with 800 mg/L GE was smooth and flat. Moreover, corrosion products were difficult to observe on the surface of N80 steel except for scratches and defects introduced during polishing.

As shown in Fig. 7a, the 3D morphology of N80 steel was exceptionally rough, and the range of the coordinate axis was wide, from -122 nm to 109.6 nm. This phenomenon showed that HCl could easily corrode N80 steel without a corrosion inhibitor.

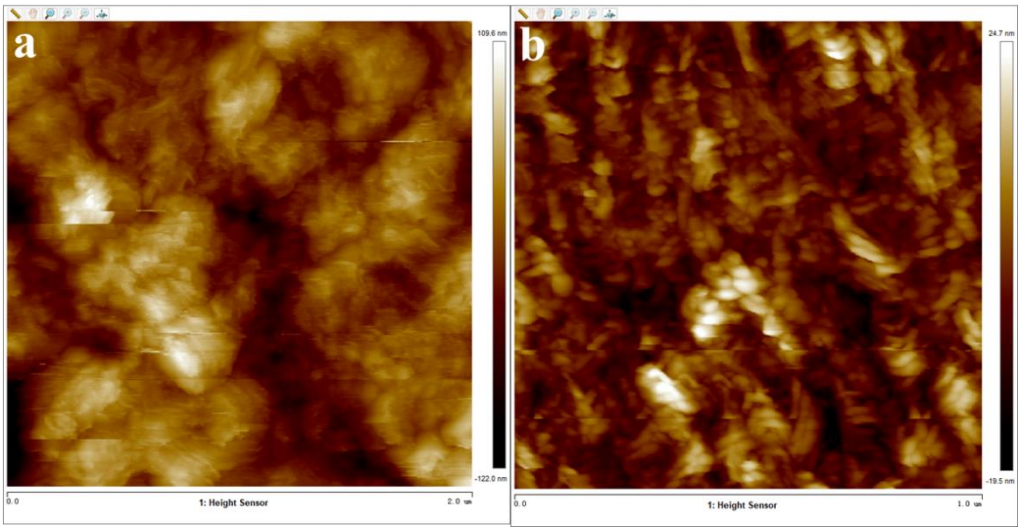

Figure 7. The AFM graphs of N80 steel in 1 M HCl solution with various concentrations of ginkgo leaf extract (0 mg/L, 800 mg/L) at 298K.

On the contrary, the corrosion degree of the N80 steel surface in Fig. 7b under the protection of 800 mg/L GE was small, and the range of the coordinate axis was narrow, from -19.5 nm to 24.7 nm. This finding could prove that the protective film formed by GE blocked the contact between the corrosive medium and the N80 steel.

3.5 Langmuir isotherm

As shown in the Langmuir isotherm of Fig. 8, the R^2 value was 0.9998 and infinitely close to 1, which implied that the adsorption of GE on the surface of N80 steel was monolayer adsorption.

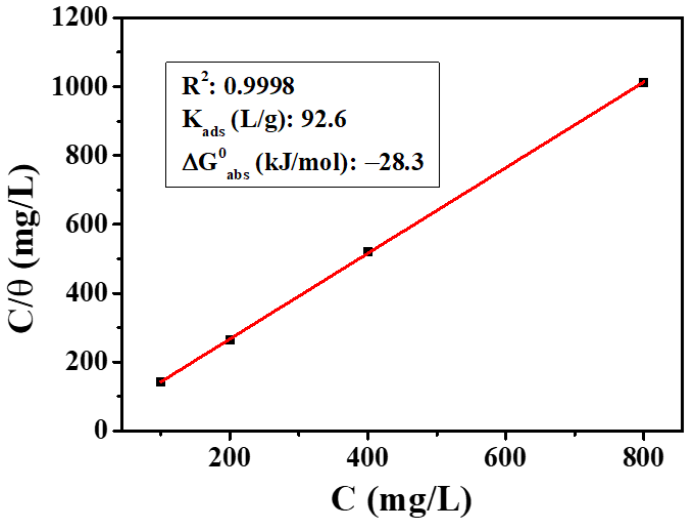

Figure 8. Langmuir adsorption isotherms and relevant thermodynamic parameters of GE on the N80 steel in 1 M HCl solution at 298 K.

That was to say, the active molecules in GE could be adsorbed on the surface of N80 steel to protect it. Based on Qiang and Li work [36, 37], two important thermodynamic parameters were calculated and given in Fig. 8. As we all know, high K_{ads} and low ΔG^0_{ads} corresponded to a strong adsorption capacity of corrosion inhibitors. In this work, the K_{ads} and low ΔG^0_{ads} values of GE were 92.6 L/g and -28.3 kJ/mol, respectively. This result showed that GE could be easily adsorbed on the surface of N80 steel and provided protection for it. The ΔG^0_{ads} value was -28.3 kJ/mol, between -20 kJ/mol (physical adsorption) and -40 kJ/mol (chemical adsorption). This finding indicated that GE showed both physical adsorption and chemical adsorption on the N80 steel surface, among which physical adsorption was dominant.

3.6 MD simulation

The molecular structure of 6-hydroxykynurenic acid (HKA) was given in Fig. 9a, HKA molecule possessed a benzene ring, four O atoms, and an N atom, which was beneficial to the adsorption of HKA on the surface of N80 steel [38, 39].

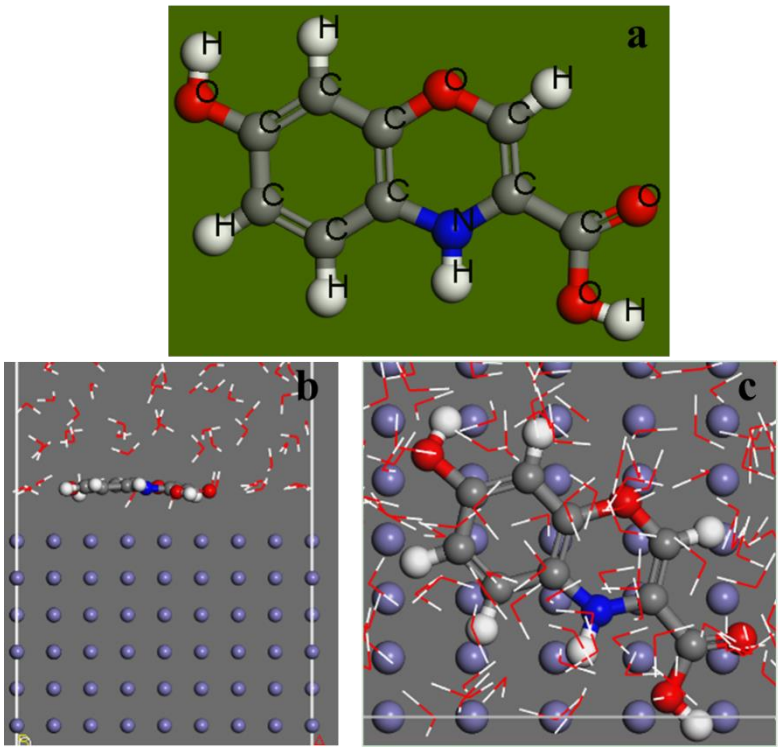

Figure 9. (a) The structure of HKA in GE, (b) equilibrium configuration side view, (c) top view of HKA.

The side and top views of equilibrium adsorption configuration were displayed in Figs 9b and 9c. It was worth noting that both the side and top views showed that HKA could be adsorbed on the Fe(110) crystal plane in parallel. This finding showed that HKA could shield the contact between the corrosive medium and the metal surface to the greatest extent and provide efficient protection for the

metal [40, 41]. This result revealed the interaction mechanism of GE and N80 steel from the microscopic level and confirmed the above experimental conclusion.

4. CONCLUSION

We prepared ginkgo leaf extract as a green corrosion inhibitor by pure water extraction in this work. We demonstrated the anti-corrosion performance of GE on N80 steel by combining experiments and calculations. The main conclusions are as follows.

1. The EIS experiments showed that GE could improve the charge transfer resistance of N80 steel in the acidic environment, which became more obvious with the increase in GE concentration from 100 mg/L to 800 mg/L.

2. Based on the Tafel polarization curve results, we found that GE could inhibit the cathodic and anodic reaction of N80 steel in 1 M HCl. Simultaneously, the inhibition of cathodic and anodic reactions became more obvious with the increase in GE concentration. Compared with blank, the self-corrosion potential change of N80 steel did not exceed 85 mV, indicating GE was a modest mixed-type corrosion inhibitor.

3. Morphological observation further proved that GE was adsorbed on the surface of N80 steel, forming a protective film to isolate the contact between the corrosive medium and N80 steel. The SEM and AFM graph results of N80 steel were consistent with the conclusions in electrochemical tests.

4. Combining Langmuir adsorption and MD, the HKA molecule was adsorbed on the surface of N80 steel through benzene rings and heteroatoms in parallel. This single-layer film provided efficient protection for N80 steel.

ACKNOWLEDGMENTS
This work is grateful for the funding of the 2021 Dongying Science Development Fund Project(DJ2021020).

References

1. Y. Qiang, S. Zhang, H. Zhao, B. Tan and L. Wang, *Corros. Sci.,* 161 (2019) 108193.
2. Y. Qiang, S. Zhang and L. Wang, *Appl. Surf. Sci.,* 492 (2019) 228-238.
3. A. Dehghani, G. Bahlakeh, B. Ramezanzadeh, A. Hossein Jafari Mofidabadi and A. Hossein Mostafatabar, *J. Colloid. Interf. Sci.,* 603 (2021) 716-727.
4. S. Eid, *Inter. J. Electrochem. Sci.,* 16 (2021) 150852.
5. S. Chen, S. Chen, H. Zhao, H. Wang, P. Wen and H. Li, *Int. J. Electrochem. Sci.,* 15 (2020) 5208-5219.
6. J. Zhang and H. Li, *Int. J. Electrochem. Sci.,* 15 (2020) 4368-4378.
7. J. Zhang and H. Li, *Int. J. Electrochem. Sci.,* 15 (2020) 5362-5372.
8. Y. Qiang, H. Zhi, L. Guo, A. Fu, T. Xiang and Y. Jin, *J. Mol. Liq.,* 351 (2022) 118638.
9. Y. Qiang, H. Li and X. Lan, *J. Mater. Sci. Technol.,* 52 (2020) 63-71.
10. J. Haque, V. Srivastava, M.A. Quraishi, D. Singh Chauhan, H. Lgaz and I.-M. Chung, *Corros. Sci.,* 172 (2020) 108665.

11. H.M. Abd El-Lateef, *Appl. Surf. Sci.,* 501 (2020) 144237.
12. S.A. Umoren, M.M. Solomon, I.B. Obot and R.K. Suleiman, *J. Ind. Eng. Chem.,* 76 (2019) 91-115.
13. C.M. Fernandes, L.X. Alvarez, N.E. dos Santos, A.C. Maldonado Barrios and E.A. Ponzio, *Corros. Sci.,* 149 (2019) 185-194.
14. G. Bahlakeh, B. Ramezanzadeh, A. Dehghani and M. Ramezanzadeh, *J. Mol. Liq.,* 283 (2019) 174-195.
15. H. Li, Y.J. Qiang, W.J. Zhao and S.T. Zhang, *Colloid. Surf. A,* 616 (2021) 126077.
16. M.H. Shahini, M. Keramatinia, M. Ramezanzadeh, B. Ramezanzadeh and G. Bahlakeh, *J. Mol. Liq.,* 342 (2021) 117570.
17. Y. Qiang, S. Zhang, B. Tan and S. Chen, *Corros. Sci.,* 133 (2018) 6-16.
18. Y. Qiang, S. Zhang, S. Yan, X. Zou and S. Chen, *Corros. Sci.,* 126 (2017) 295-304.
19. B. Tan, S. Zhang, H. Liu, Y. Guo, Y. Qiang, W. Li, L. Guo, C. Xu and S. Chen, *J. Colloid. Interf. Sci.,* 538 (2019) 519-529.
20. H. Li, S.T. Zhang and Y.J. Qiang, *J. Mol. Liq.,* 321 (2021) 114450.
21. H. Li, Y. Qiang, W. Zhao and S. Zhang, *Corros. Sci.,* 191 (2021) 109715.
22. Y. Zhang, M. Nie, X. Wang, Y. Zhu, F. Shi, J. Yu and B. Hou, *J. Hazard. Mater.,* 289 (2015) 130-139.
23. M. Bobina, A. Kellenberger, J.-P. Millet, C. Muntean and N. Vaszilcsin, *Corros. Sci.,* 69 (2013) 389-395.
24. S. Varvara, G. Caniglia, J. Izquierdo, R. Bostan, L. Găină, O. Bobis and R.M. Souto, *Corros. Sci.,* 165 (2020) 108381.
25. Z.B. Wang, H.X. Hu and Y.G. Zheng, *Corros. Sci.,* 130 (2018) 203-217.
26. H. Tian, Y.F. Cheng, W. Li and B. Hou, *Corros. Sci.,* 100 (2015) 341-352.
27. R. Álvarez-Bustamante, G. Negrón-Silva, M. Abreu-Quijano, H. Herrera-Hernández, M. Romero-Romo, A. Cuán and M. Palomar-Pardavé, *Electrochim. Acta,* 54(23) (2009) 5393-5399.
28. Y. Yan, W. Li, L. Cai and B. Hou, *Electrochim. Acta,* 53(20) (2008) 5953-5960.
29. V. Rajeswari, D. Kesavan, M. Gopiraman, P. Viswanathamurthi, K. Poonkuzhali and T. Palvannan, *Appl. Surf. Sci.,* 314 (2014) 537-545.
30. N.A. Odewunmi, S.A. Umoren and Z.M. Gasem, *J. Environ. Chem. Eng*., 3 (2015) 286-296.
31. P.E. Alvarez, M.V. Fiori-Bimbi, A. Neske, S.A. Brandán and C.A. Gervasi, *J. Ind. Eng. Chem.,* 58 (2018) 92-99.
32. S.A. Umoren, Z.M. Gasem and I.B. Obot, *Ind. Eng. Chem. Res.,* 52 (2013) 14855-14865.
33. B.X. Vuong, T.L. Huynh, T.Q.N. Tran, S.V.P. Vattikuti, T.D. Manh, P. Nguyen-Tri, A.T. Nguyen, P. Van Hien and N. Nguyen Dang, *Mater. Today Commun.,* 31 (2022) 103641.
34. F.A. Zakaria, T.S. Hamidon and M.H. Hussin, *J. Indian Chem. Soc.,* 99 (2022) 100329.
35. H. Qian, D. Zhang, Y. Lou, Z. Li, D. Xu, C. Du and X. Li, *Corros. Sci.,* 145 (2018) 151-161.
36. Y. Qiang, L. Guo, H. Li and X. Lan, *Chem. Eng. J.,* 406 (2021) 126863.
37. H. Li, S. Zhang, B. Tan, Y. Qiang, W. Li, S. Chen and L. Guo, *J. Mol. Liq.,* 305 (2020) 112789.
38. W. Gong, X. Yin, Y. Liu, Y. Chen and W. Yang, *Prog. Org. Coat.,* 126 (2019) 150-161.
39. L. Ma, Y. Qiang and W. Zhao, *Chem. Eng. J.,* 408 (2021) 127367.
40. Y Zhang, Y Qiang, H Ren, J Cao, L Cui, Z Zong, D Chen and T Xiang, *Prog. Org. Coat.,* 170 (2022) 106971.
41. Y. Qiang, S. Zhang, S. Xu and W. Li, *J. Colloid Interf. Sci.,* 472 (2016) 52–59